Electronic Supplementary Material (ESI) for New Journal of Chemistry.

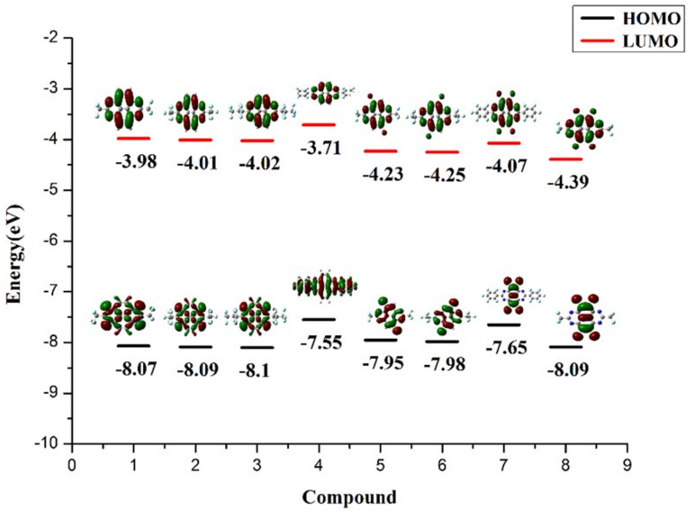

Fig S1. Calculated pictorial representations and energies of HOMOs and LUMOs of TAPy derivatives 1-8 at the B3LYP/6-31+G(d,p)

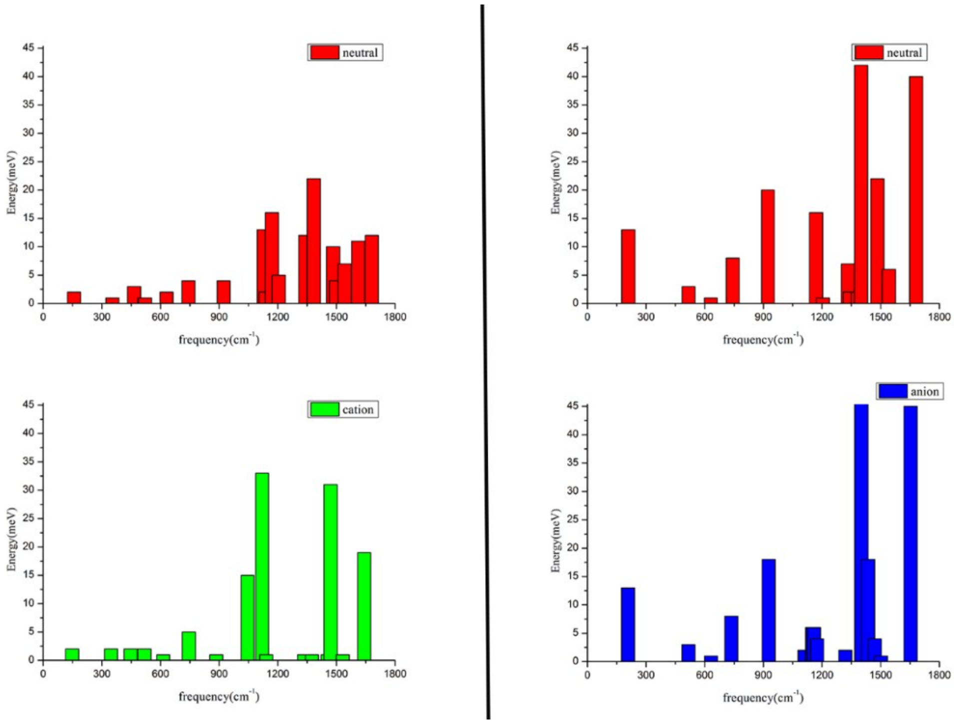

Fig S2. The vibrational frequencies contributions to the intramolecular reorganization energies of 1 neutral (top), anion and cation (bottom) by means of the B3LYP/6-31+G (d,p) calculation.

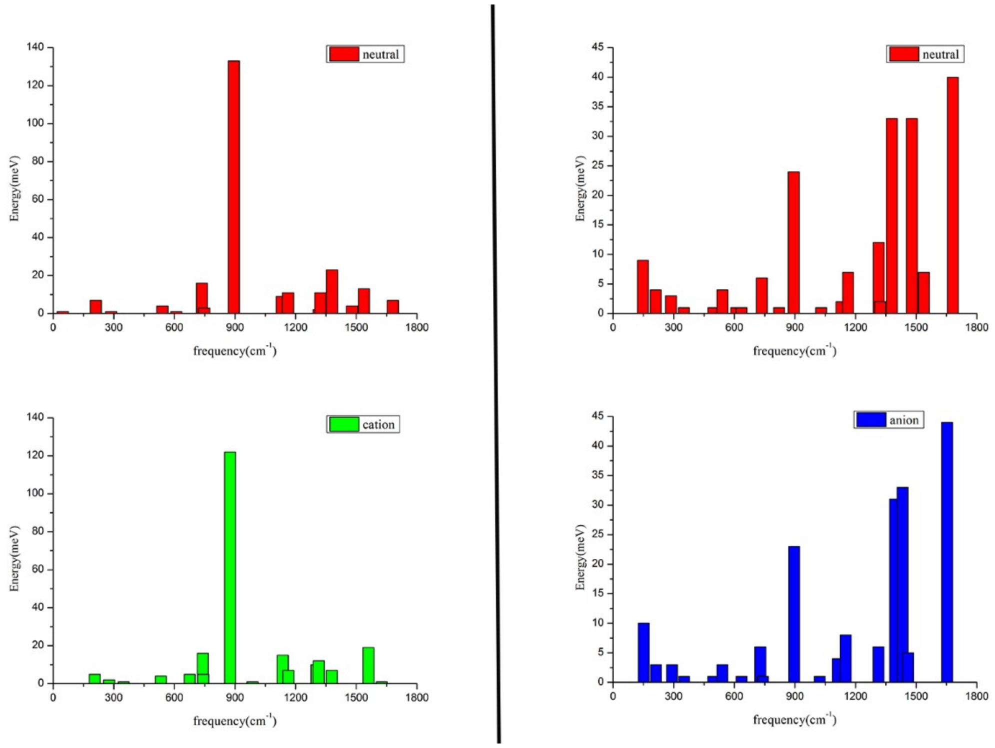

Fig S3. The vibrational frequencies contributions to the intramolecular reorganization energies of 2 neutral (top), anion and cation (bottom) by means of the B3LYP/6-31+G (d,p) calculation.

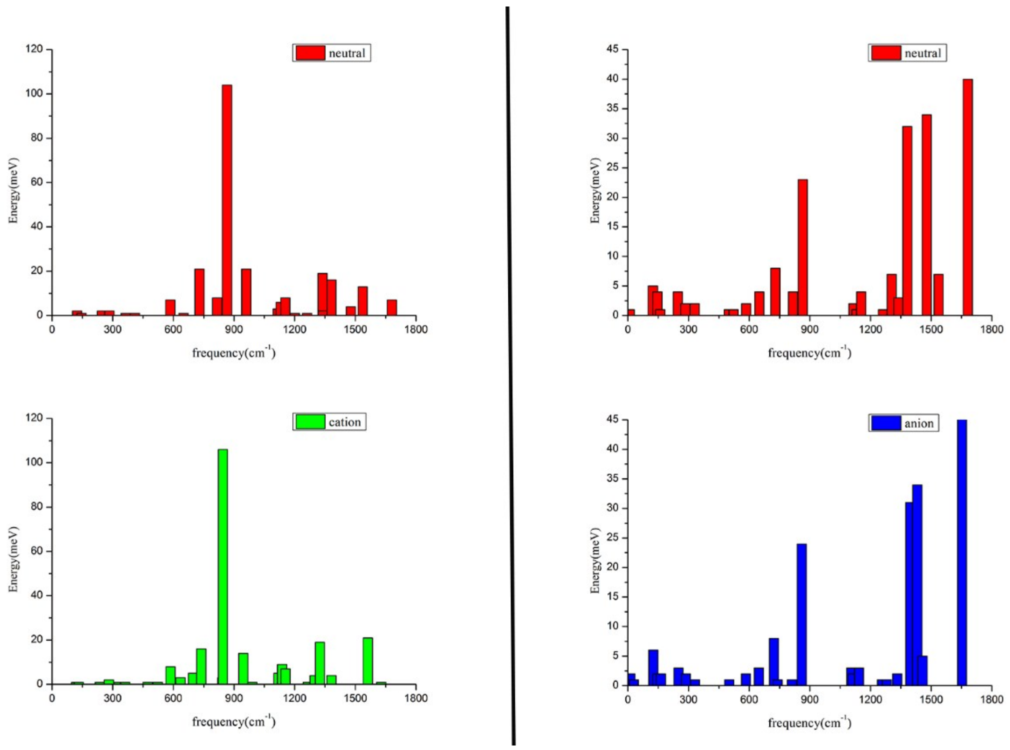

Fig S4. The vibrational frequencies contributions to the intramolecular reorganization energies of 3 neutral (top), anion and cation (bottom) by means of the B3LYP/6-31+G (d,p) calculation.

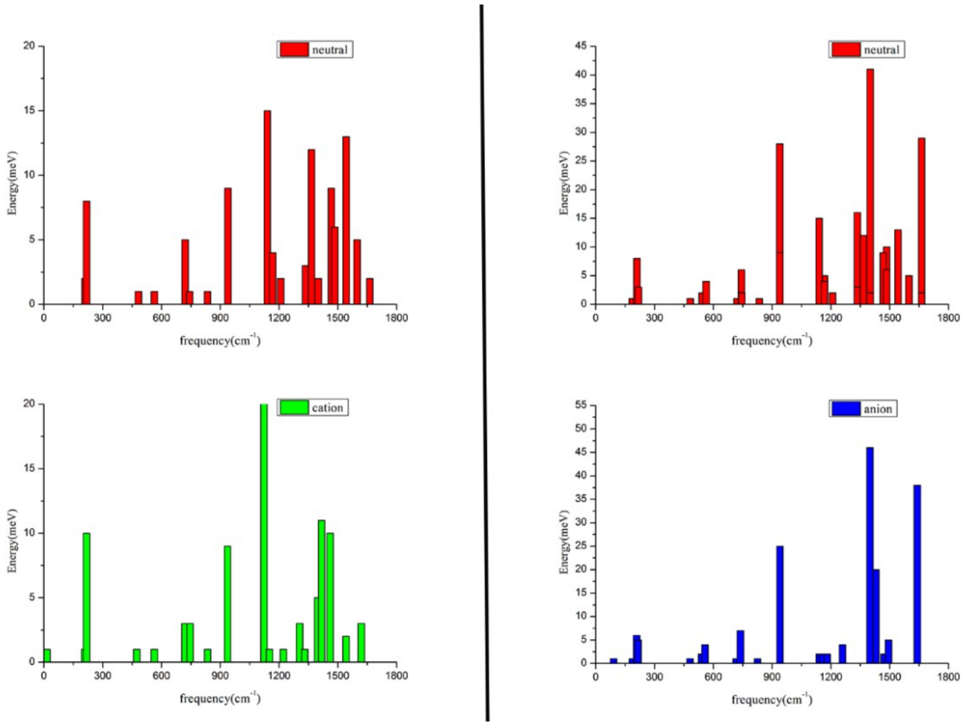

Fig S5. The vibrational frequencies contributions to the intramolecular reorganization energies of 5 neutral (top), anion and cation (bottom) by means of the B3LYP/6-31+G (d,p) calculation.

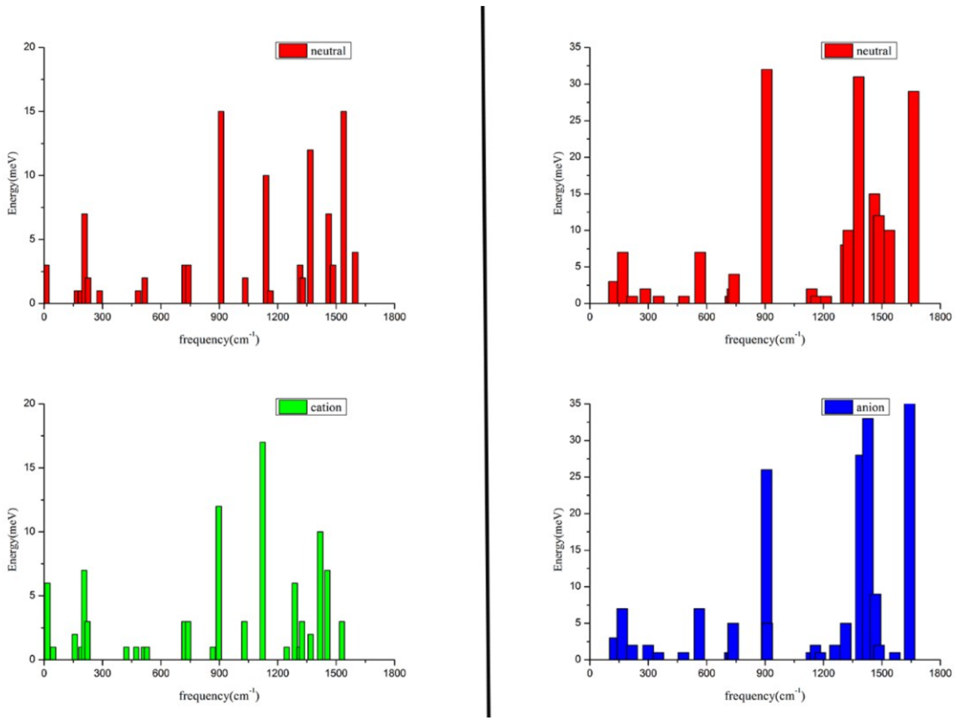

Fig S6. The vibrational frequencies contributions to the intramolecular reorganization energies of 6 neutral (top), anion and cation (bottom) by means of the B3LYP/6-31+G (d,p) calculation.

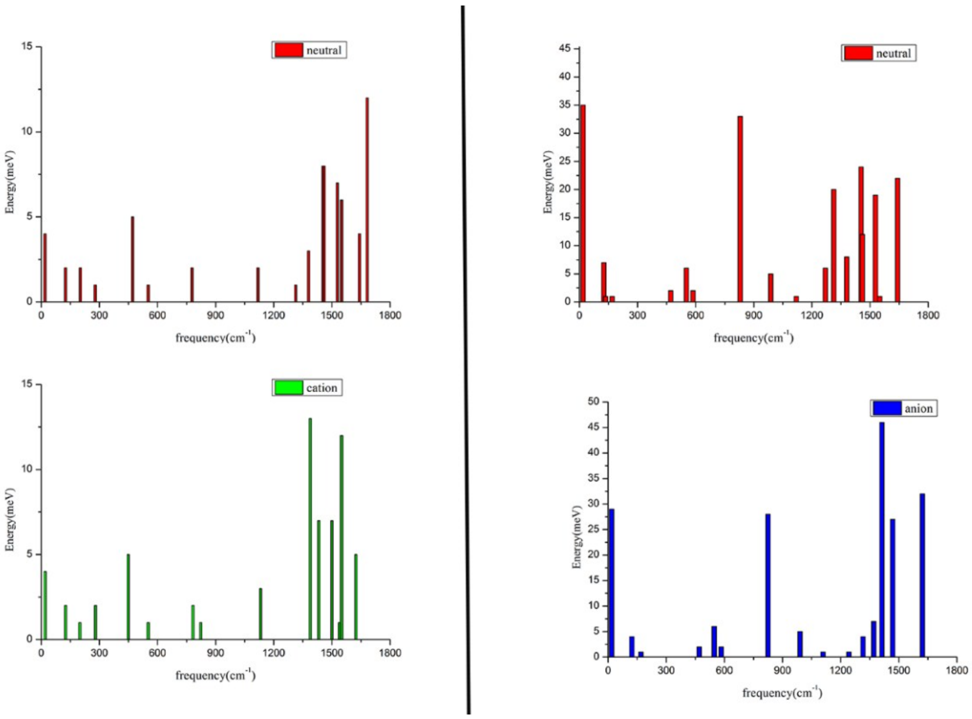

Fig S7. The vibrational frequencies contributions to the intramolecular reorganization energies of 7 neutral (top), anion and cation (bottom) by means of the B3LYP/6-31+G (d,p) calculation.

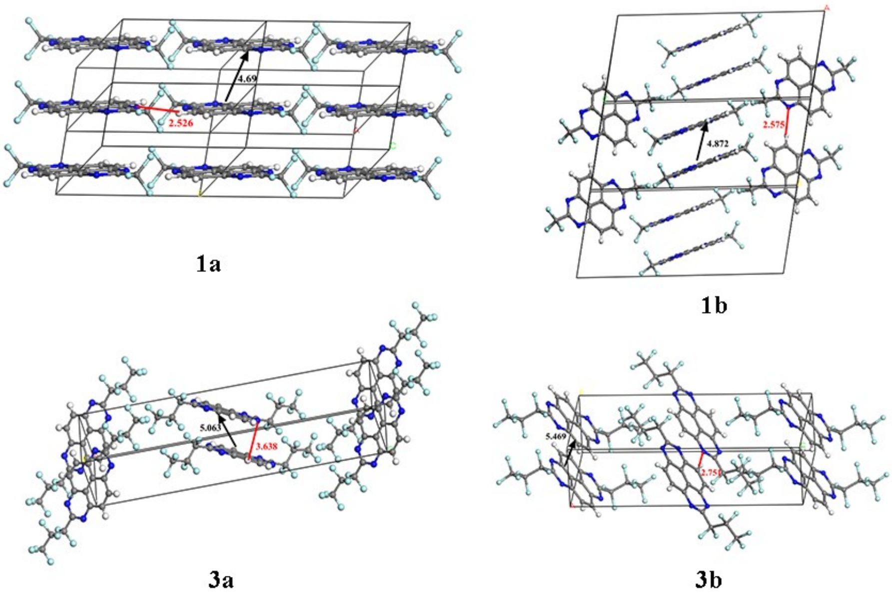

Fig S8. Crystal structures of two polymorphs of compounds 1 and 3

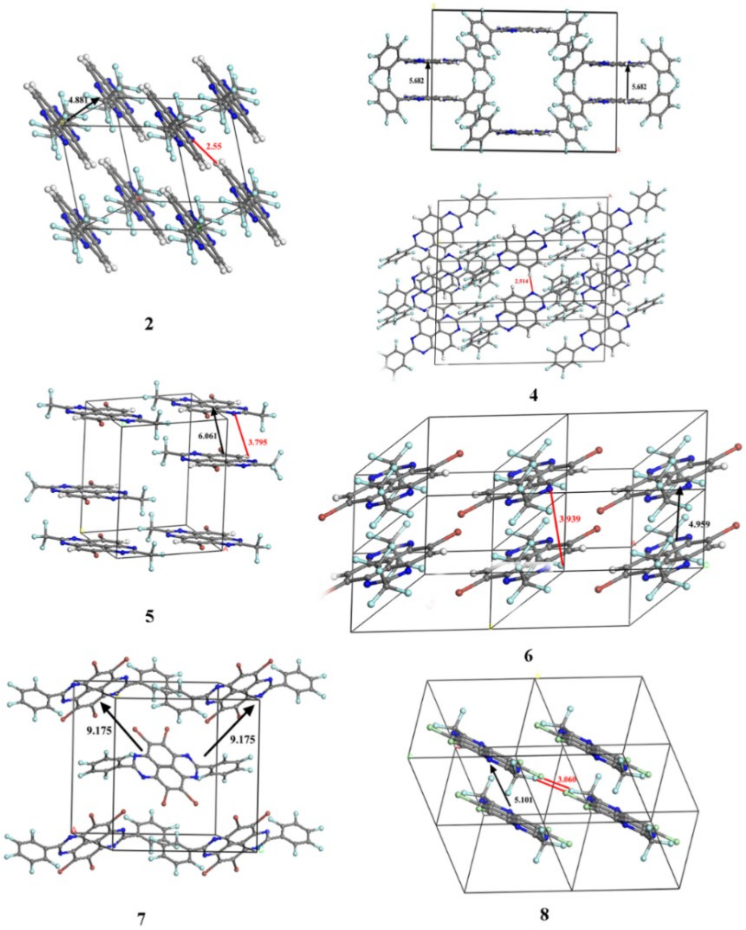

Fig S9. Crystal structures of compound 2, 4, 5, 6, 7, and 8

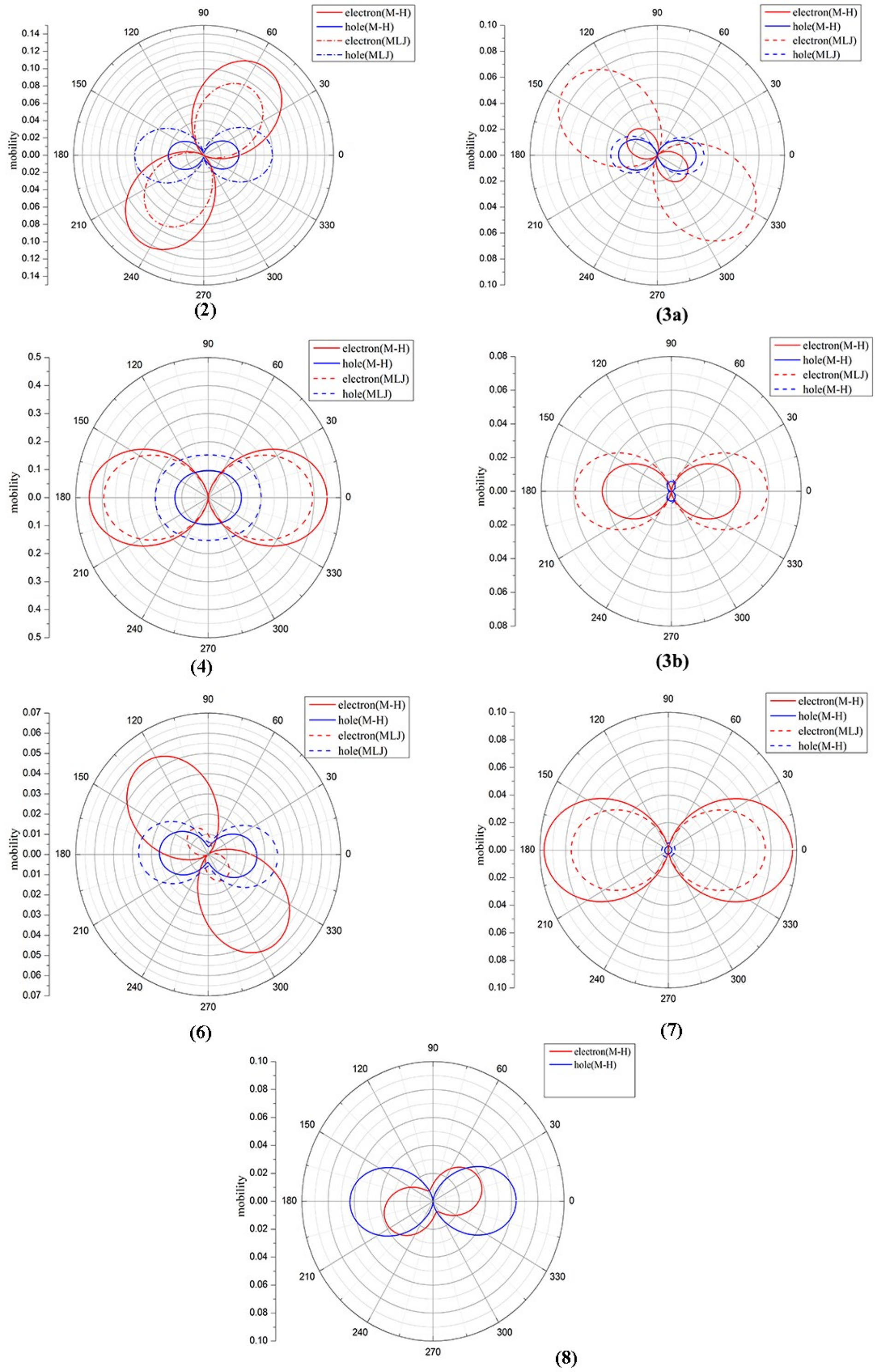

Fig S 10. Predicted anisotropic mobilities obtained in the a–b plane in the single crystals for TAPy derivatives 2-8

Table S1 Absolute energies of the neutral and charged species employed to evaluate the intramolecular reorganization energies according to the AP method along with vertical and adiabatic EAs.

b3pw91/6-	$E^0(G^0)$	$E^+(G^+)$	$E^-(G^-)$	$E^+(G^0)$	$E^-(G^0)$	$E^0(G^+)$	$E^0(G^-)$

311+g(d,p)							
1	-1353.84702	-1353.48783	-1353.9446	-1353.4835	-1353.9379	-1353.84185	-1353.842619
2	-1829.38369	-1829.02376	-1829.48377	-1829.01256	-1829.4768	-1829.37936	-1829.376798
3	-2304.91395	-2304.56662	-2305.01511	-2304.55751	-2305.00797	-2304.90422	-2304.906698
4	-2134.08269	-2133.76189	-2134.17641	-2133.75582	-2134.16883	-2134.07637	-2134.075204
5	-6500.89006	-6500.54487	-6501.00083	-6500.54137	-6500.99420	-6500.88619	-6500.88350
6	-6976.42680	-6976.08129	-6976.53953	-6976.07772	-6976.53271	-6976.4226	-6976.42005
7	-12428.1619	-12427.8409	-12428.2749	-12427.83830	-12428.2678	-12428.1591	-12428.15496
8	-3192.09701	-3191.74877	-3192.2139	-3191.74451	-3192.20732	-3192.0926	-3192.090262
b3lyp/6-31+g(d,p)	$E^0(G^0)$	$E^+(G^+)$	$E^-(G^-)$	$E^+(G^0)$	$E^-(G^0)$	$E^0(G^+)$	$E^0(G^-)$
1	-1354.06100	-1353.70615	-1354.15607	-1353.7021	-1354.14939	-1354.05621	-1354.054388
2	-1829.65161	-1829.30481	-1829.74924	-1829.28366	-1829.74236	-1829.65623	-1829.644796
3	-2305.23702	-2304.89075	-2305.33573	-2304.88233	-2305.32865	-2305.22773	-2305.230044
4	-2134.41727	-2134.09686	-2134.50855	-2134.09093	-2134.50103	-2134.41119	-2134.409992
5	-6496.30818	-6495.96635	-6496.41655	-6495.96291	-6496.41999	-6496.30439	-6496.301683
6	-6971.89943	-6971.55719	-6972.00988	-6971.55374	-6972.00315	-6971.8956	-6971.892764
7	-12418.9139	-12418.5941	-12419.0245	-12418.5917	-12419.0174	-12418.9113	-12418.90697
8	-3191.77701	-3191.41877	-3191.8939	-3191.42451	-3191.89732	-3191.7636	-3191.761262

Table S2. Effective frequency ω_{eff} and associated HR factor S_{eff} employed in the evaluation of charge transfer rate constants of 1-7 (B3LYP/6-31G*)

		1	2	3	4	5	6	7
S_{eff}	hole	0.949	3.721	3.808	1.878	1.936	1.688	2.986
W_{eff}		2141	1040	1044	1456	825	970	1094
λ_{class}		0.004	0.012	0.008	0.035	0.021	0.031	0.016
S_{eff}	electron	2.133	1.759	2.269	1.970	1.458	1.980	3.141
W_{eff}		1369	1710	1361	1608	1969	1487	1040
λ_{class}		0.026	0.026	0.031	0.040	0.023	0.026	0.078

Table S3. Charge transfer rate constants calculated by the semiclassical Marcus-Hush and quantum-corrected Marcus-Levich-Jortner models (in s^{-1})

		W_{h-MH}	W_{e-MH}	W_{h-MLJ}	W_{e-MLJ}
1a/xy	1	6.817×10^{12}	2.647×10^{8}	2.021×10^{13}	3.003×10^{8}
	2	6.472×10^{10}	1.034×10^{10}	1.918×10^{11}	1.173×10^{10}
	3	4.190×10^{11}	2.680×10^{12}	1.242×10^{12}	3.041×10^{12}
	4	7.991×10^{8}	4.485×10^{7}	2.368×10^{9}	5.066×10^{7}
yz	5	4.190×10^{11}	2.680×10^{12}	1.242×10^{12}	3.041×10^{12}
	6	3.328×10^{5}	3.376×10^{7}	9.864×10^{5}	3.831×10^{7}
	7	5.668×10^{11}	1.118×10^{10}	1.680×10^{12}	1.269×10^{11}
	8	2.995×10^{6}	4.136×10^{6}	8.878×10^{6}	4.693×10^{6}
xz	9	6.817×10^{12}	2.553×10^{8}	2.021×10^{13}	3.003×10^{8}
	10	3.954×10^{9}	1.284×10^{10}	1.172×10^{10}	1.457×10^{10}
	11	5.668×10^{11}	1.112×10^{10}	1.685×10^{12}	1.262×10^{10}
	12	2.609×10^{8}	8.440×10^{6}	7.733×10^{8}	9.577×10^{7}

1b/xy	1	3.567×10^{11}	2.433×10^{12}	1.202×10^{12}	2.761×10^{12}
	2	2.927×10^{5}	1.426×10^{7}	9.864×10^{5}	1.618×10^{8}
	3	3.755×10^{12}	1.155×10^{9}	1.266×10^{13}	1.310×10^{9}
	4	1.223×10^{13}	2.28×10^{9}	4.122×10^{13}	2.301×10^{9}
yz	5	3.567×10^{11}	2.433×10^{12}	1.202×10^{12}	2.761×10^{12}
	6	6.324×10^{9}	5.403×10^{9}	2.132×10^{10}	6.130×10^{9}
	7	1.717×10^{12}	2.235×10^{9}	3.946×10^{12}	4.805×10^{9}
	8	1.725×10^{9}	2.110×10^{6}	4.297×10^{9}	2.394×10^{6}

Table S4. Calculated center-of-mass distances (in Å), charge transfer integrals (in meV) and charge transfer rate constants (in s^{-1}) for all possible hopping channels by the semiclassical Marcus-Hush and quantum-corrected Marcus-Levich-Jortner models.

		θ	s	V_{ije}	V_{ijh}	$W_{h\text{-}MH}$	$W_{e\text{-}MH}$	$W_{h\text{-}MLJ}$	$W_{e\text{-}MLJ}$
2	1	0.00	7.116	28.87	-5.43	5.96×10^{11}	1.28×10^{10}	1.16×10^{12}	9.72×10^{9}
	2	54.64	8.534	10.23	-45.45	7.49×10^{10}	8.95×10^{11}	1.46×10^{11}	6.81×10^{11}
	3	88.65	4.881	-16.22	2.08	1.88×10^{11}	1.87×10^{9}	3.66×10^{11}	1.43×10^{9}
	4	123.53	8.723	0.03	0.11	6.44×10^{5}	5.24×10^{6}	1.25×10^{6}	3.99×10^{6}
3a	1	0.00	6.776	25.38	-4.93	3.91×10^{11}	4.05×10^{9}	4.70×10^{11}	5.66×10^{9}
	2	36.77	8.459	0.19	-0.07	2.19×10^{5}	8.17×10^{5}	2.63×10^{7}	1.14×10^{6}
	3	90.00	5.063	-0.22	1.26	2.94×10^{7}	2.65×10^{8}	3.53×10^{7}	3.70×10^{8}
	4	143.23	8.459	10.45	35.01	6.63×10^{10}	2.04×10^{11}	7.96×10^{10}	6.52×10^{11}
3b	1	0.00	8.662	6.37	41.9	2.46×10^{10}	2.93×10^{11}	2.96×10^{10}	4.09×10^{11}
	2	32.27	10.244	0.15	-0.21	1.37×10^{7}	7.35×10^{6}	1.64×10^{7}	1.03×10^{7}
	3	90.00	5.469	-14.11	-0.62	1.21×10^{11}	6.41×10^{7}	1.45×10^{11}	8.95×10^{7}
	4	147.73	10.244	-0.35	1.8	7.44×10^{7}	5.40×10^{8}	8.93×10^{7}	7.54×10^{8}
4	1	0.00	8.561	-8.32	53.63	3.45×10^{10}	3.20×10^{12}	5.49×10^{10}	2.81×10^{12}
	2	41.12	5.682	-84.57	-3.95	3.57×10^{12}	1.74×10^{10}	5.68×10^{12}	1.52×10^{10}
	3	138.84	5.682	-84.5	-3.91	3.56×10^{12}	1.70×10^{10}	5.67×10^{12}	1.49×10^{10}
6	1	0.00	4.959	29.68	-4.6	6.88×10^{11}	9.94×10^{10}	9.83×10^{11}	2.76×10^{10}
	2	69.80	8.895	0.01	-0.03	7.81×10^{4}	4.23×10^{6}	1.12×10^{5}	1.18×10^{6}
	3	102.74	8.559	-14.14	4.75	1.56×10^{11}	1.06×10^{11}	2.23×10^{11}	4.95×10^{10}
	4	129.36	10.797	7.61	8.91	4.52×10^{10}	3.73×10^{11}	6.46×10^{10}	1.04×10^{11}
7	1	0.00	12.987	-0.19	6.2	2.37×10^{7}	3.80×10^{11}	4.55×10^{7}	2.97×10^{11}
	2	44.95	9.175	-7.28	2.34	3.47×10^{10}	5.42×10^{10}	6.69×10^{10}	4.23×10^{10}
	3	135.05	9.175	-7.12	2.42	3.32×10^{10}	5.80×10^{10}	6.39×10^{10}	4.53×10^{10}
8	1	0.00	5.101	-40.24	-14.99	1.35×10^{12}	7.93×10^{11}	-	-
	2	48.04	10.35	-10.78	-9.98	9.70×10^{10}	3.52×10^{11}	-	-
	3	76.70	7.908	-4.06	5.24	1.38×10^{10}	9.69×10^{10}	-	-
	4	113.10	8.366	0.36	-0.02	1.08×10^{8}	1.41×10^{6}	-	--